Biochimica et Biophysica Acta 1837 (2014) 1707–1716

Contents lists available at ScienceDirect

Biochimica et Biophysica Acta

journal homepage: www.elsevier.com/locate/bbabio

Modeling the respiratory chain complexes with biothermokinetic equations — The case of complex I

Margit Heiske [a,b,d,1], Christine Nazaret [c], Jean-Pierre Mazat [a,d,*]

[a] Université de Bordeaux, Bordeaux, France
[b] Institut für Biologie Theoretische Biophysik Humboldt-Universität zu Berlin, Invalidenstraße 42, Berlin, Germany
[c] Institut de Mathématiques de Bordeaux, ENSTBB-Institut Polytechnique de Bordeaux, France
[d] Laboratoire de métabolisme énergétique cellulaire, IBGC — CNRS UMR 5095, 1 Rue Camille Saint Saëns, 33077 Bordeaux, France

ARTICLE INFO

Article history:
Received 5 January 2014
Received in revised form 9 July 2014
Accepted 16 July 2014
Available online 24 July 2014

Keywords:
Complex I
Oxidative phosphorylation
Modeling

ABSTRACT

The mitochondrial respiratory chain plays a crucial role in energy metabolism and its dysfunction is implicated in a wide range of human diseases. In order to understand the global expression of local mutations in the rate of oxygen consumption or in the production of adenosine triphosphate (ATP) it is useful to have a mathematical model in which the changes in a given respiratory complex are properly modeled. Our aim in this paper is to provide thermodynamics respecting and structurally simple equations to represent the kinetics of each isolated complexes which can, assembled in a dynamical system, also simulate the behavior of the respiratory chain, as a whole, under a large set of different physiological and pathological conditions. On the example of the reduced nicotinamide adenine dinucleotide (NADH)–ubiquinol–oxidoreductase (complex I) we analyze the suitability of different types of rate equations. Based on our kinetic experiments we show that very simple rate laws, as those often used in many respiratory chain models, fail to describe the kinetic behavior when applied to a wide concentration range. This led us to adapt rate equations containing the essential parameters of enzyme kinetic, maximal velocities and Henri–Michaelis–Menten like-constants (K_M and K_I) to satisfactorily simulate these data.

1. Introduction

The respiratory chain plays a crucial role in energy metabolism. In many cases, it consists of four enzyme complexes which are connected through two electron transporters, ubiquinone and cytochrome *c*. Three of the respiratory complexes extrude protons from the mitochondrial matrix into the intermembrane space liberating, step by step, the energy of the transfer of electrons from the low redox potential of the substrates NADH or $FADH_2$ to the high redox potential of oxygen, energy then used to synthesize ATP.

It is now well documented that respiratory chain dysfunction is responsible for a wide range of human diseases including neurodegenerative diseases and cancer. Respiratory chain dysfunction may also have a possible relationship with aging [1,2] and metabolic disorders [3]. In many cases respiratory chain dysfunctions are due to mutations in the subunit constituting the respiratory chain complexes.

In order to better understand the behavior of the respiratory chain in different physiological conditions and how the effects of pathological mutations are expressed at the global level of oxygen consumption or ATP synthesis it is useful to have a theoretical model of the respiratory chain. In other words understanding the normal or pathological interplay between these complexes and the electron transporters in the global functioning of the respiratory chain requires a model of each respiratory complex with a specific rate equation and then the integration of all the rate equations into a dynamical system representing the operation of the whole oxidative phosphorylation.

Several models, with different levels of complexity, have been established to describe the respiratory chain or its isolated complexes. It does not enter the scope of this article to review them all. We would just like to analyze the way in which the behavior of each individual respiratory complex is approached in these models of the whole respiratory chain. It means that we discard of our analysis all the models in which the respiratory chain is represented by only one or two (depending on the electron entry point) equations (typically Magnus and Keizer [4], Cortassa et al. [5] and many others). Among the remaining models of respiratory chain two types of modeling of the individual complexes are used. The first significant models were developed in the framework of the Non-Equilibrium Thermodynamic model (NET) involving a linear dependence of the flux as a function of the thermodynamic forces [6–9]. The model developed by Korzeniewski and Froncisz [10,11], is a

* Corresponding author at: IBGC-CNRS, 1, rue Camille Saint-Saëns, 33077 Bordeaux cedex, France.
E-mail address: jpm@u-bordeaux2.fr (J.-P. Mazat).
[1] Present address: Laboratoire d'Anthropologie Moléculaire et Imagerie de Synthèse, AMIS — CNRS UMR 5288, Université Paul Sabatier Toulouse III, 37 Allées Jules Guesde, 31073 Toulouse cedex3, France.

http://dx.doi.org/10.1016/j.bbabio.2014.07.013
0005-2728/

comprehensive model also well representative of this class of thermodynamic models, extended thereafter ([12,13]).

Another approach, largely used to model the isolated respiratory complexes is the Mass Action Law (MAL), with the forward rate proportional to the product of substrates and the backward proportional to the product of products of the reaction. Bohnensack [14] was probably the first to derive a quantitative model of the respiratory chain involving nearly all the components of oxidative phosphorylation. In this approach the respiratory complexes were modeled according to the Mass-Action law. A recent example of this approach was proposed by Beard [15].

The advantage of both approaches (NET and MAL) is that they use very simple rate laws for each of the complexes with only one parameter to adjust. But these equations cannot reflect the respiratory complexes' behaviors over a wide range of physiological conditions as it will be shown later in this paper.

As a matter of fact, the behavior of the individual complexes is rather complex for several reasons: (i) the mechanisms catalyzed by each separate complex are complex in themselves. The most illustrating example is the Q-cycle operating in complex III with two different quinone binding sites and the bifurcation of the electrons coming from the QH_2 molecule into two pathways. The case of cytochrome *c* oxidase (complex IV) also involves a complex synchronization between the 4 electrons necessary to reduce oxygen in water and the protons pumping. The case of complex I is not yet entirely resolved but already includes a cascade of 7 or 8 elementary redox reactions. (ii) Not only substrates, products and modifiers play a role in the kinetics but also the electrochemical proton gradient which has an important influence on the activity of each complex and thus on the whole respiratory chain. (iii) The regulation of the activity of these complexes depends on allosteric conformations or on chemical modifications such as phosphorylation and acetylation [16–19].

On the one hand, the derivation of equations describing very precisely the underlying mechanisms of the respiratory complexes often involves a huge number of parameters which are hard or impossible to determine experimentally and will be in any case underdetermined [20,21]. On the other hand, the experimental kinetics of these complexes show, most of the time, the traditional pattern of enzymatic kinetics *i.e.* saturation behavior. Furthermore, the recorded kinetics have been analyzed with the usual phenomenological approaches of enzymology, particularly with the determination of V_{max}, K_M and K_I at least for some of the substrates or products. It is well illustrated in the measurement of the (maximal) activity of the individual complexes, which is particularly useful in the diagnosis of mitochondrial diseases in attributing at least in some cases the pathology to a particular defect in a given complex as in [22]. In the same time the activity of the whole respiratory chain (and of part of TCA cycle) is recorded classically in very different conditions (resting state with a maximal transmembrane proton potential (state 4), phosphorylating state with a lower proton potential (state 3), intermediate states between states 4 and 3, uncoupled state *etc.*). In all these physiological conditions, the concentrations of the substrates/products of the individual respiratory complexes (NAD/NADH, Q/QH_2, redox state of Cyt *c*) are also very different and presumably also different from the concentrations used in the determination of the (maximal) activity of the individual complexes. This could invalidate the use of the parameter values determined in these latter conditions (maximal activity determination in the absence of products) for the modeling of the whole respiratory chain functioning at nonmaximal activity in the presence of products.

For this reason we studied the kinetics of the isolated respiratory complexes in a broad range of substrate/product concentrations with the first aim to integrate the observations in a rate equation as simple as possible but nevertheless illustrating the main characteristics of the kinetics, particularly the saturation behavior, the presence of products and the thermodynamic constraints. Our aim is to use these "simple" rate equations both to model kinetics of the individual isolated complexes and also the global behavior of the whole respiratory chain when all the respiratory complexes are considered together. We will analyze different types of equations already used (NET, MAL) and we will propose other equations [23–27], more able to fit the kinetics of respiratory complexes particularly when involved in electron transport and proton translocation through the whole respiratory chain: Extended Reversible Henri–Michaelis–Menten Equation (ER-HMM), Ping Pong Mechanism (PPM), Ordered Mechanism (OM), "Convenience Kinetics" (CK) and a new type of equation: Extended Mass Action (EMA) (Table 1 and Fig. 1). As an example, we will compare all these equations in their ability to model our kinetic results already published in [28] on beef heart complex I (NADH–Coenzyme Q reductase activity). It catalyzes the reaction:

$$NADH + H^+ + Q <==> NAD^+ + QH_2. \quad (1)$$

2. Materials and methods

2.1. Preparation of mitochondria

Frozen isolated beef heart mitochondria were a gift from Dr. Joel Lunardi, prepared according to [29]. In this preparation the final mitochondrial pellets were homogenized at a concentration of 40 mg/mL and the mitochondrial suspension was frozen in liquid nitrogen as small beads of 50 μL volume and stored at −80 °C. In our experiments, one bead was thawed and diluted (1/5), aliquoted and the aliquots are frozen again. Then for each experiment an aliquot is thawed and diluted once more (1/20) in the slightly hypo-osmotic reaction buffer in order to ensure that the membranes are broken and their potential is null. For the assay itself, the mitochondrial suspension was diluted again (final concentration: 4.4 μg mitochondrial proteins in 1 mL). All assays were performed in a temperature-controlled single wavelength spectrophotometer.

Table 1
The different equations discussed in this paper. *Ordered of binding: NADH,Q, and of release:. NAD, QH2.

Name and abbreviation	Equation	Equilibrium constraints
Extended Reversible Henri–Michaelis–Menten (ER-HMM equation)	$v = E_t \cdot \frac{k_f \frac{NADH}{K_{NADH}} \frac{Q}{K_Q} - k_b \frac{NAD}{K_{NAD}} \frac{QH_2}{K_{QH_2}}}{\left(1+\frac{NADH}{K_{NADH}}+\frac{NAD}{K_{NAD}}\right)\left(1+\frac{Q}{K_Q}+\frac{QH_2}{K_{QH_2}}\right)}$	$K_{eq} = \frac{k_f}{k_b} \cdot \frac{K_{NAD}}{K_{NADH}} \cdot \frac{K_{QH_2}}{K_Q}$
Convenience Kinetics (CK equation)	$v = E_t \cdot \frac{k_f \frac{NADH}{K_{NADH}} \frac{Q}{K_Q} - k_b \frac{NAD}{K_{NAD}} \frac{QH_2}{K_{QH_2}}}{\left(1+\frac{NADH}{K_{NADH}}\right)\left(1+\frac{Q}{K_Q}\right)+\left(1+\frac{NAD}{K_{NAD}}\right)\left(1+\frac{QH_2}{K_{QH_2}}\right)-1}$	$K_{eq} = \frac{k_f}{k_b} \cdot \frac{K_{NAD}}{K_{NADH}} \cdot \frac{K_{QH_2}}{K_Q}$
Extended Mass Action Equation (EMA equation)	$v = E_t \cdot \frac{k_f \frac{NADH \cdot Q}{C_S} - k_b \frac{NAD \, QH_2}{C_P}}{1+\frac{NADH \cdot Q}{C_S}+\frac{NAD \, QH_2}{C_P}}$	$K_{eq} = \frac{k_f}{k_b} \cdot \frac{C_P}{C_S}$
Ordered Mechanism * OM(NQNQ) equation	$v_{OM} = E_t \cdot \frac{k_f \frac{NADH}{K_{NADH}} \frac{Q}{K_Q} - k_b \frac{NAD}{K_{NAD}} \frac{QH_2}{K_{QH2}}}{\left[\begin{array}{l} 1 + \frac{NADH}{K_{NADH}} + \frac{Q}{K_Q} + \frac{NAD}{K_{NAD}} + \frac{QH_2}{K_{QH2}} + \frac{NADH}{K_{NADH}} \cdot \frac{Q}{K_Q} + \frac{NAD}{K_{NAD}} \cdot \frac{QH_2}{K_{QH2}} + \\ \frac{NADH}{K_{NADH}} \cdot \frac{QH_2}{K_{QH2}} + \frac{Q}{K_Q} \cdot \frac{NAD}{K_{NAD}} + \frac{NADH}{K_{NADH}} \cdot \frac{Q}{K_Q} \cdot \frac{NAD}{K_{NAD}} + \frac{Q}{K_Q} \cdot \frac{NAD}{K_{NAD}} \cdot \frac{QH_2}{K_{QH2}} \end{array}\right]}$	$K_{eq} = \frac{k_f}{k_b} \cdot \frac{K_{NAD}}{K_{NADH}} \cdot \frac{K_{QH_2}}{K_Q}$
Ping-Pong Mechanism PPM equation	$v_{PPM} = E_t \cdot \frac{k_f \frac{NADH}{K_{NADH}} \frac{Q}{K_Q} - k_b \frac{NAD}{K_{NAD}} \frac{QH_2}{K_{QH2}}}{\left[\begin{array}{l} \frac{NADH}{K_{NADH}} + \frac{Q}{K_Q} + \frac{NAD}{K_{NAD}} + \frac{QH_2}{K_{QH2}} + \frac{NADH}{K_{NADH}} \cdot \frac{Q}{K_Q} + \\ \frac{NAD}{K_{NAD}} \cdot \frac{QH_2}{K_{QH2}} + \frac{NADH}{K_{NADH}} \cdot \frac{NAD}{K_{NAD}} + \frac{Q}{K_Q} \cdot \frac{QH_2}{K_{QH2}} \end{array}\right]}$	$K_{eq} = \frac{k_f}{k_b} \cdot \frac{K_{NAD}}{K_{NADH}} \cdot \frac{K_{QH_2}}{K_Q}$

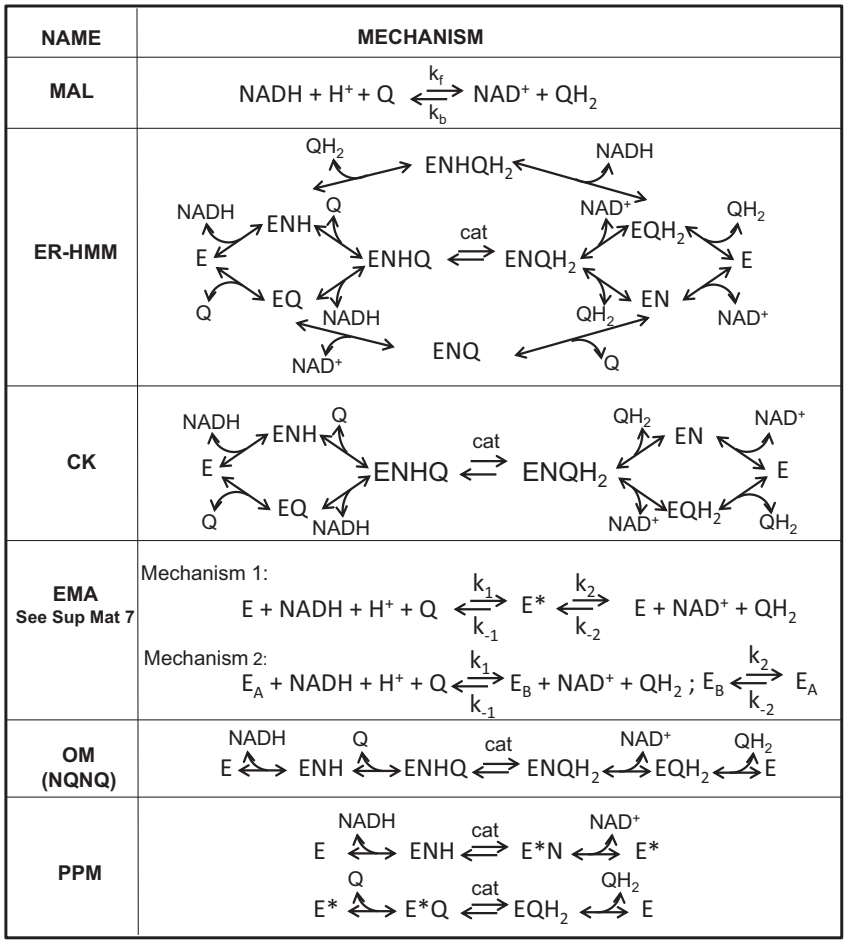

Fig. 1. Mechanisms associated to the rate equations. MAL means Mass Action Law. In ER-HMM (Extended Reversible-Henri–Michaelis–Menten) and in CK (convenience Kinetics) mechanisms, ENH means E-NADH, ENHQ: E-NADH-Q, $ENHQH_2$: E–NADH–QH_2, ENQ: E–NAD–Q, $ENQH_2$: E–NAD–QH_2, EQH_2: E–QH_2 and EN: E–NAD. In EMA mechanism 1, E* symbolizes an Enzyme–Substrates–Product complex. In mechanism 2, E_A and E_B represent two enzyme conformations able to bind respectively the substrates only and the products only. The derivations of the EMA equation are detailed in Supplementary materials 2.

2.2. Complex I (NADH–ubiquinone oxidoreductase) assay

The assay was performed at 37 °C according to [22] by following the decrease in absorbance at 340 nm resulting from the oxidation of NADH in 1 mL of medium containing 65 mM KH_2PO_4 (pH 7.5), 2 mg BSA, 2 mM EDTA, 46 μM antimycin A, 4.4 μg mitochondrial protein and in control assays additionally 25 μM rotenone. A constant ethanol concentration of 8 μL/1000 μL was present in all assays. It means that the complement to this quantity was added when not brought by the added constituents. The concentrations of the substrates NADH and Q (decylubiquinone) are varied, as well as the concentrations of products NAD^+ and QH_2. The reaction was initiated by NADH addition. The extinction coefficient used for NADH concentration determination was 6.22 mM^{-1} cm^{-1} at 340 nm. The net activities have been obtained by subtracting the residual activity in the presence of rotenone from the activities without.

2.3. Parameter estimations

The parameter values of the different rate equations have been estimated minimizing the root mean square deviation (RMSD) between the experimental and theoretical data points. RMSD for one set of parameters was calculated simultaneously with all experimental series (see figures in the Supplementary materials). To find the RMSD minimum, we used a global search routine (genetic algorithm) followed by a local one (quasi Newton based) as proposed in [30]. It permits to browse the whole parameter space and then to converge toward a well defined solution, usually unique in our cases. All calculations have been done using Scilab (Scilab Enterprises, 2012 http://www.scilab-enterprises.com/). Because the reaction catalyzed by the respiratory chain complex I is highly exergonic, the rate constant of the backward reaction k_b is simply calculated *via* the Haldane relationship:

$$K_{eq} = \frac{k_f}{k_b} \cdot \frac{K_{NAD}}{K_{NADH}} \cdot \frac{K_{QH_2}}{K_Q} \tag{2}$$

or equation

$$K_{eq} = \frac{k_f}{k_b} \cdot \frac{C_P}{C_S} \tag{3}$$

for EMA with the equilibrium constant:

$$K_{eq} = \exp\left(-\frac{\Delta G'_o}{RT}\right) = 1.54 \times 10^{+11} \tag{4}$$

where R = 8.314 J/mol/K. The temperature in the experiments was T = 310 K and $\Delta G'o = -66.4$ kJ/mol at pH 7.5 (69.4 at pH 7.0).

Table 2
Fits of the experimental points by the different saturable equations of Table 1.
The kinetic parameters are identified by minimizing the root mean square deviation (RMSD) calculated between all experimental data and the corresponding theoretical points evaluated with the equation under study as explained in the Materials and methods section (see Supplementary materials for the figures of all fits). The k_b value has been calculated using the Haldane relationship with $K_{eq} = 1.5410^{11}$ corresponding to $\Delta G'_o$ (pH 7.5; T = 310 K) = −66.4 kJ/mol.

Equation	RMSD	k_f	k_b	K_{NADH}	K_Q	K_{NAD}	K_{QH2}
	[nmol NADH·min^{-1}·mg^{-1}]			[μM]	[μM]	[μM]	[μM]
PPM	162	1910	$1.3\cdot10^{-6}$	6.1	13.1	2064	4.0
OM (NQNQ)	161	1802	$1.0\cdot10^{-5}$	4.4	9.9	13,931	2.7
OM (QNQN)	162	1797	$5.0\cdot10^{-6}$	4.3	9.8	774	23.6
OM (QNNQ)	164	1801	$1.9\cdot10^{-5}$	4.4	9.7	13,087	5.3
OM (NQQN)	168	1793	$9.2\cdot10^{-6}$	4.3	9.8	1666	20.1
ER-HMM	164	1791	$1.1\cdot10^{-6}$	4.3	9.7	780	5.3
CK	167	1773	$1.5\cdot10^{-8}$	4.2	9.5	88	0.6
EMA	244	1333	$1.8\cdot10^{-10}$	$C_S = 166\ \mu M^2$		$C_P = 3.4\ \mu M^2$	

3. Results

3.1. Non-saturable rate equations

3.1.1. Near Equilibrium Thermodynamics (NET) equation

In the near equilibrium approach the reaction velocity is assumed to be proportional to the Gibbs energy.

$$v_{CI} = -k_{CI} \cdot \Delta G_{CI} \tag{5}$$

with:

$$\Delta G_{CI} = \Delta G'_{o,CI} + RT \cdot Ln\left[\frac{[NAD]\cdot[QH_2]}{[NADH]\cdot[Q]}\right]. \tag{6}$$

This type of equation was proposed by Westerhoff [7] and used by Korzeniewski et al. [10] for instance to model complexes I and III of the respiratory chain.

3.1.2. The Mass Action Law equation

The MAL equation applied to the enzymatic reaction (1) reads:

$$v_{CI} = k_f[NADH]\cdot[Q] - k_b[NAD]\cdot[QH_2] \tag{7}$$

or introducing K_{eq}:

$$v_{CI} = k_b\left(K_{eq}[NADH]\cdot[Q] - [NAD]\cdot[QH_2]\right). \tag{8}$$

This type of equation was largely used for modeling the respiratory chain complexes (*e.g.* [14,15]).

We conclude that these equations (see supplementary material 1), MAL as well as the NET equation cannot be used for an accurate description of respiratory complex kinetics when there is a possible variation in substrate and product concentrations. It is necessary to introduce a saturation term in the rate equations.

3.2. The saturable rate equations

3.2.1. The equations

The list of the rate equations tested in this work which exhibit a saturable pattern as a function of substrate or product concentrations is given in Table 1 and their mechanisms are depicted in Fig. 1. They all involve the same type of numerator as MAL equation vanishing at equilibrium (or an equivalent expression in the case of EMA). In addition, they also involve a denominator with Michaelis constants K_M for substrates and products. Because we look for an equation as simple as possible we assume that the K_M for a substrate/product is independent of the binding of the others which is not necessarily true in reality. Because the denominators of the equations are different, one can predict that the values of K_M may be different for the different equations. All these equations but PPM are equivalent in the absence of products.

The Extended-Reversible Henri–Michaelis–Menten (ER-HMM) equation [23–25,31–34] corresponds to a random binding/release of substrates/products as represented in Fig. 1. It is well described in all textbooks (see [26] for instance).

The Convenience Kinetics equation (CK) is a generic equation which can account for any number of substrates and products. It has been proposed by Liebermeister and Klipp [27] and includes the same basic kinetic parameters (linked by the same Haldane relationship) as the ER-HMM equation above but arranged slightly differently in the denominator so that the K_M values may be different. In the case of 2 substrates 2 products, it also corresponds to a random binding mechanism but, in contrast to the ER-HMM mechanism, it is without the non-reactive ternary complexes E–NADH–QH_2 and E–NAD–Q (see Fig. 1).

The interests of the ER-HMM equation is well explained by Cornish–Bowden and Hofmyer in [23] which also applies to CK: a minimal number of parameters, adherence to thermodynamic constraints, competition between substrates and their corresponding products and saturability.

The equation given in Table 1 for the order mechanism (OM) correspond to the case NQNQ meaning that NADH binds first then Q and NAD is released first then QH_2. The four possible sequences of substrate binding/product release have been tested (see Table 2).

A ping-pong mechanism was also proposed for complex I kinetics (see the discussion in [28]). It can correspond to two situations: NNQQ or QQNN meaning that either NADH reacts first and gives NAD and then Q gives QH_2 or *vice versa*. In the simplified form where the K_M are independent of each other, both equations have the same expression given in Table 1.

Finally we tested the EMA equation (Extended Mass Action) which is based on mass action according to two different possible mechanisms (see supplementary material 2 for a complete derivation of this equation). It can also be seen as a simplified ER-HMM equation in which the Michaelis constants of the substrates (resp. the products) are fused in one constant C_S (resp. C_P). The equation has only 4 parameters which are not independent; one can be replaced by the equilibrium constant *via* the Haldane-like relationship (3)

This equation has the big advantage that any stoichiometric factor (also non integer) can be included, like for the NET and MAL equations. This equation was developed independently by Liebermeister et al. [35].

For each equation, the results of parameter fitting using all the experimental points are listed in Table 2. Fig. 2e to h gives an example of these fittings in the case of ER-HMM and EMA equation with only some of the experimental points. The figures showing the results of the fittings according to other saturable rate laws with the complete set of experimental points are shown in the Supplementary materials. The results are always plotted in comparison with the ER-HMM fit (blue dashed).

Comparing the RMSD (Table 2), it is clear that all equations but EMA give nearly the same good accuracy. The rate constants and the substrate K_M values are also very similar (except for EMA for which the parameters have different meanings). An average value of $k_f = 1\,810 \pm 43$ nmol·min^{-1}·prot^{-1}, $K_{NADH} = 4.6 \pm 0.7$ μM and $K_Q = 10.2 \pm 1.3$ μM are obtained. This is not the case for the K_M values of the

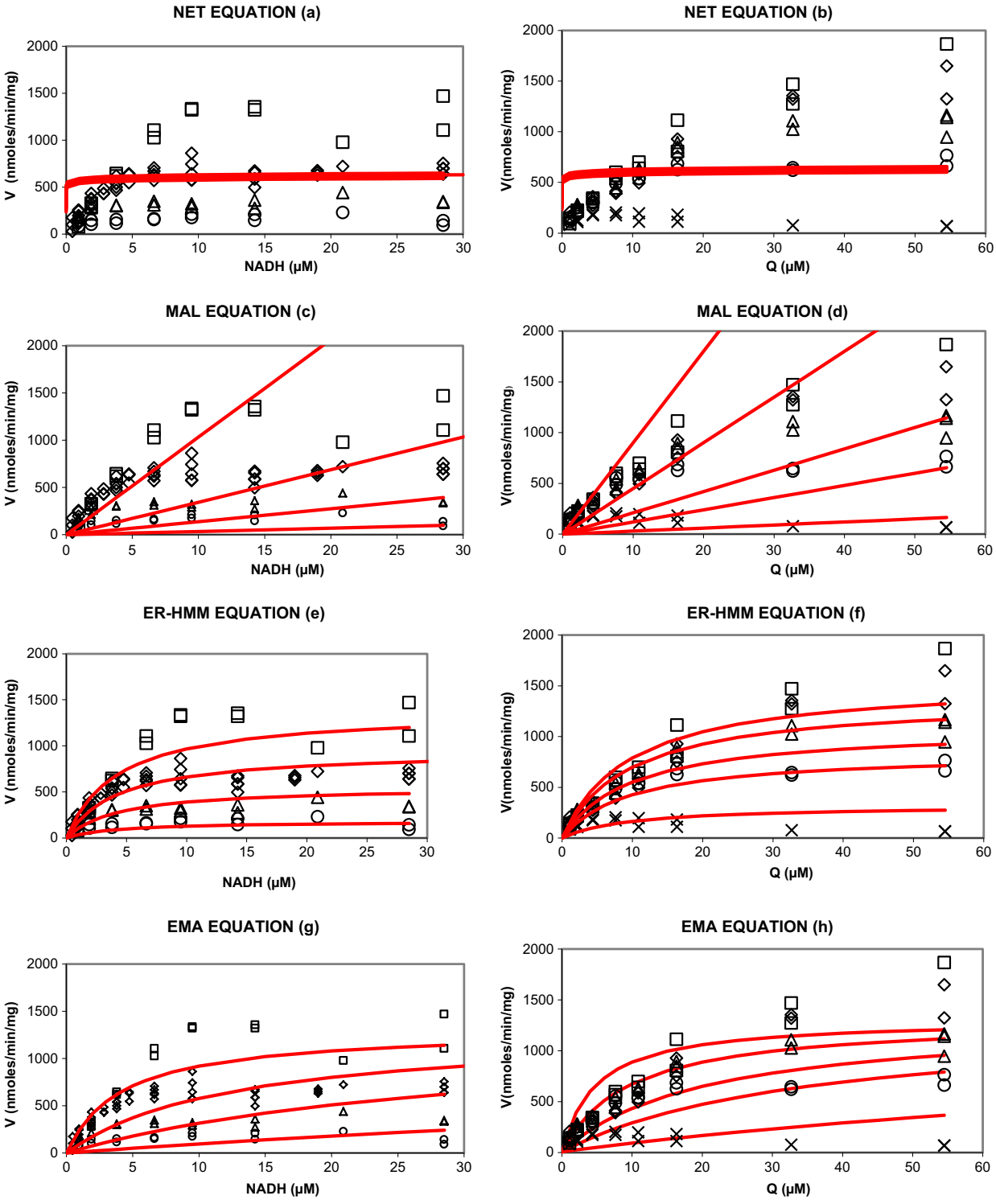

Fig. 2. Comparison of different rate equations to fit part of the experimental results. The kinetic parameters are determined by minimizing the root mean square deviation (RMSD) calculated between all experimental data and the corresponding theoretical points evaluated with the equation under study (see Table 1) as explained in the Materials and methods section. Note that the fitting procedure is performed on all experimental results represented in the Supplementary materials, but that only a small part of them is represented in this comparison for clarity. The experimental points are in black and the fitting curves in red. (a and b): The experimental points are fitted by the NET equation. (c and d): The experimental points are fitted by the MAL equation. (e and f): The experimental points are fitted by the ER-HMM equation. (g and h): The experimental points are fitted by EMA equation. The parameters for tracing the theoretical curves are listed in Table 1. Other parameters. NET: $k_{cl} = 6.6$ nmol·min^{-1}·mg^{-1}; MAL: $k_f = 3.16$ nmol·(μM)$^{-2}$·min^{-1}·mg^{-1}; $k_b = 2.04\,10^{-11}$ nmol·(μM)$^{-2}$·min^{-1}·mg^{-1}. NADH variable: (○) Q = 1.1 μM; (△) Q = 4.4 μM; (◊) Q = 10.9 μM; (□) Q = 32.7 μM. Q variable: (X) NADH = 0.95 μM; (○) NADH = 3.8 μM; (△) NADH = 6.65 μM; (◊) NADH = 14.25 μM; (□) NADH = 28.5 μM.

products. The determination of the products K_M is more difficult because as mentioned above, the complex I reaction is largely irreversible in the absence of $\Delta\mu_H^+$. The only way to have an indication of the products K_M is to record the reaction rate in the forward direction in the presence of different concentrations of the products (Fig. 3). The values of the products K_M are dependent on the structure of the denominator of each equation, but still one can state that K_{NAD} is clearly high and difficult to measure indicating a low affinity of NAD^+. On the other hand K_{QH2} is rather low, sometimes lower than K_Q. Both K_M products depend upon the rate equation used to fit the experimental results.

3.2.2. Q inhibition

Fig. 4 shows a clear inhibition at high Q concentration (>100 μM). Different types of substrate inhibitions can be considered such as non-competitive, substrate/steric inhibition (at the normal binding site). On the example of ER-HMM equation, several inhibition terms have been tested. The ER-HMM equation reads then:

$$v = E_t \cdot I_{nc} \cdot \frac{k_f \cdot \frac{NADH}{K_{NADH}} \cdot \frac{Q}{K_Q} - k_b \cdot \frac{NAD}{K_{NAD}} \cdot \frac{QH_2}{K_{QH_2}}}{\left(1 + \frac{NADH}{K_{NADH}} + \frac{NAD}{K_{NAD}}\right)\left(1 + \frac{Q}{K_Q} I_s + \frac{QH_2}{K_{QH_2}} I_s\right)} \quad (9)$$

with the inhibition terms I_s and I_{nc} described in the following.

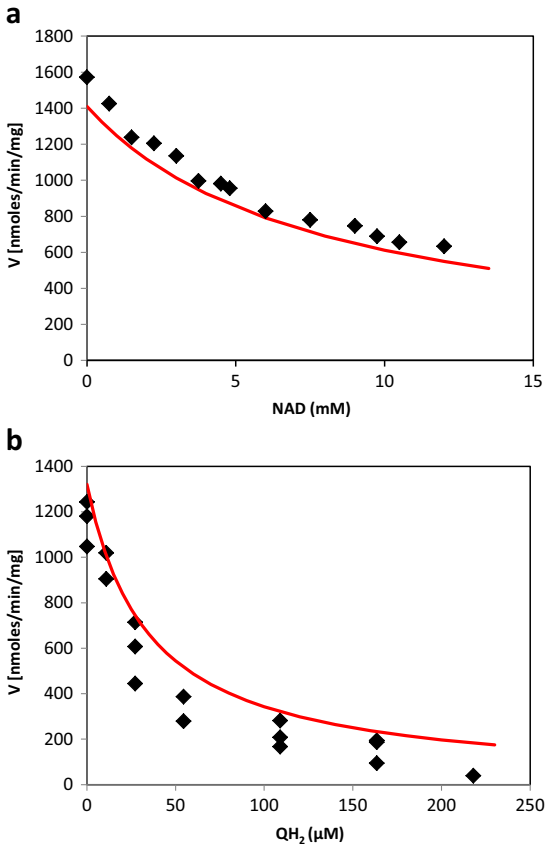

Fig. 3. Product inhibition. a: NAD inhibition with NADH = 38 μM and Q = 69 μM. (See also figures z to ac in the Supplementary materials. This figure corresponds to figure ac with the ER-HMM equation.) b: QH_2 inhibition with NADH = 28.5 μM and Q = 54.5 μM. (See also figures v and w in the Supplementary materials. This figure corresponds to figure w with ER-HMM equation.) The fitting curve is represented by a continuous red line.

3.2.2.1. Substrate-product or steric inhibition I_s. This type of inhibition corresponds to the obstruction of the catalytic site of quinone reduction by quinone or quinol. Assuming that Q and QH_2 obstruction has the same effect on the binding of both molecules QH_2 or Q, the term I_s can be written:

$$I_S = 1 + \frac{[Q]}{K_{i1}} + \frac{[QH_2]}{K_{i2}} \quad (10)$$

where K_{i1} and K_{i2} are the inhibition constants of Q and QH_2 respectively. In the case where $K_{i1} = K_{i2} = K_i$, the expression (10) becomes:

$$I_S = 1 + \frac{[Q_{tot}]}{K_i} \quad \text{where} \quad [Q_{tot}] = [Q] + [QH_2]. \quad (11)$$

3.2.2.2. Noncompetitive inhibition I_{nc}. Another possibility is that Q or/and QH_2 bind to a second quinone site on the molecule, modifying the activity of complex I, giving rise to a non-competitive inhibition.

The generic expression of a non-competitive inhibition is:

$$I_{nc} = \left(\frac{1}{1 + \frac{[Q]}{K_{i1}} + \frac{[QH_2]}{K_{i2}}}\right)^n. \quad (12)$$

The values n = 1 and n = 2 have been tested with inhibition by Q_{tot} (with $K_{i1} = K_{i2} = K_i$) or Q alone.

All the experimental points have been fitted by ER-HMM Eq. (9) involving different I_s or I_{nc} terms listed in Table 3 (see supplementary materials Figs. 7 and 8).

Very similar accuracies of the different fits are obtained. In the case of steric inhibition, taking Q and QH_2 separately or Q_{tot} as an inhibitor makes no real difference (not shown). It is the same in the case of non-competitive inhibition. In this latter case taking n = 1 or n = 2 gives similar fits. The steric (red broad line) and non-competitive (black thin line) inhibitions are represented on Fig. 4 and overlap. The curve without inhibition (blue dashed line) is also shown for comparison. Interestingly the values of K_Q (and of K_{NADH}) remain approximately the same for all types of inhibition. Only K_{QH2} changes significantly when part of the normal (product) QH_2 inhibition is taken by the specific inhibitory mechanism.

4. Discussion and conclusion

4.1. NET and MAL rate equations

As obvious in Fig. 2 (a to d), Near Equilibrium Thermodynamics (NET) and Mass Action Law (MAL) rate equations fail to adequately represent the activity of complex I when the concentrations of substrates are varied. In the case of NET, the logarithmic term dampens the variations of substrate concentrations so that the rate value is nearly constant (between 540 and 650 $nmol \cdot min^{-1} \cdot mg \cdot prot^{-1}$) over the nearly two order of magnitude of substrate concentrations used. Only at a very low concentration of one substrate, the rate decreases rapidly toward zero (in fact to minus infinity; see the red line along the y-axis in Fig. 2a and b). It is not surprising because in conditions of very low product concentrations (0.1 μM each in our case to make the calculation possible) with a value of $\Delta G'_o = -66.4$ kJ, the reaction is far from equilibrium and its rate will not obey the conditions of near Equilibrium Thermodynamics.

A slightly better fit is obtained with the MAL equation, because in this case the rate equation is sensitive to substrate concentration variations. However the linear increase of the rate as a function of substrate concentrations does not correspond to the reality of saturable kinetics.

For comparison the fit of the same points with a typical saturable kinetic equation (ER-HMM, Fig. 2e–f) is shown. However NET and MAL equations may be a good choice for the description of the respiratory chain in conditions close to equilibrium which can be the case

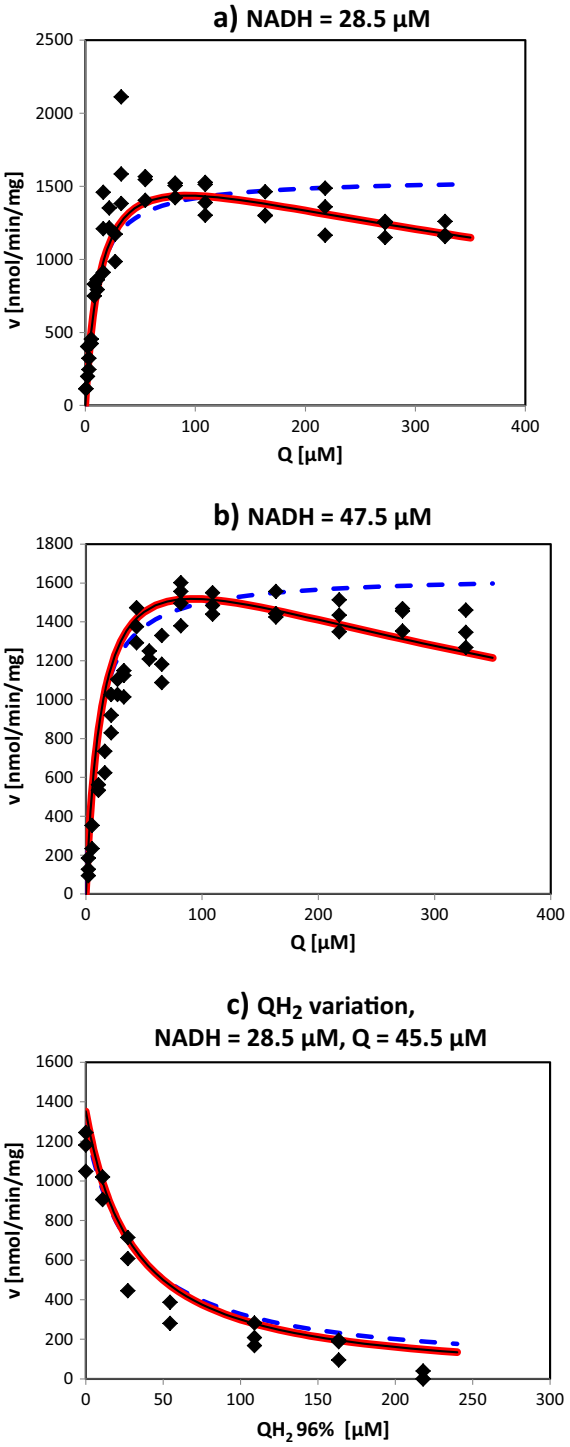

Fig. 4. Complex I inhibition by the substrate Q. The curves are drawn according to the ER-HMM equation (Eq. 13) with the parameters of Table 2 in the absence of Q substrate inhibition (- - -) and with the term $I_s = 1 + Q/K_I$ (red large line) with the parameters of Table 3, second row ($k_f = 2194$, $K_{NADH} = 4.5$ µM, $K_Q = 14.7$ µM, $K_{NAD} = 743$ µM, $K_{QH2} = 7.5$ µM and $K_I = 576$ µM) or with the term $I_{nc} = 1/(1 + Q/K_I)$ (thin black line overlapped by the red one) with the parameters of Table 3, third row ($k_f = 2254$, $K_{NADH} = 4.5$ µM, $K_Q = 15.1$ µM, $K_{NAD} = 743$ µM, $K_{QH2} = 7.6$ µM and $K_I = 561$ µM). The black diamonds correspond to the experimental points at (a) NADH = 28.5 µM, (b) NADH = 47.5 µM. (c) depicts the rate as a function of QH_2 with NADH = 28.5 µM and Q = 45.5 µM with steric inhibition (▬) or noncompetitive inhibition (___ superimposed with the previous one ▬) or without any inhibition (- - -). The fits of the other inhibitory function are very similar (not shown). See also Figs. S5 and S6 in Supplementary materials.

for complexes I, II and III of respiratory chain in *in vivo* conditions with $\Delta\mu_H^{\cdot} \neq 0$. It must be stressed that in all cases, the constants involved in these equations (k_{CI} or k_f) get *ad hoc* values which do not correspond to any intrinsic property (kinetic constants) of the respiratory complexes. Nevertheless, as demonstrated by Pillay et al. [36], a MAL model can give rise to a "saturation" behavior particularly in redox cycles when the sum of the redox couples (NAD/NADH and Q/QH_2) is constant. In these conditions, the maximal velocity depends upon the rate constant and the total concentrations of substrates/products and the half saturation concentration also depends upon the total concentration of the redox couples and is thus variable and different from a real K_M. Using such equations will make it difficult to analyze the effect on OXPHOS of a variation of a particular kinetic parameter (k_{cat} or K_M) of a given respiratory complex or of physiological or pathological changes in total substrate and product concentrations.

On the contrary Fig. 2e–h (and Figs. 3 to 8 in the Supplementary materials) and Table 2 show that all the other equations tested in our study give similar good fits when compared with the whole set of our experimental data. It should be however noticed that the EMA fit, which involves two parameters less, is less accurate mainly because it does not have independent saturation terms for each of the substrates/products. Their binding is rather considered simultaneous (see the Supplementary materials) and quantified by the phenomenological constants C_S and C_P. When the K_M of substrates (respectively the products) are similar the phenomenological constants C represent adequately their association by an average constant. It is no longer the case when the K_M are different as here for NAD and NADH.

4.2. Kinetic mechanism and kinetic constants

The striking result of this study that several kinetic equations are equally able to fit the experimental results over large concentrations of substrates and products is consistent with the fact that the kinetic mechanism of this reaction is still a matter of discussion. It means that this form of analysis does not shed light on the, too complex, kinetic mechanism of the reaction. Fato et al. [37] proposed a ping-pong mechanism in the case of mitochondria isolated from bovine heart with the oxidation of NADH preceding the reduction of ubiquinone. Nakashima et al. [38] used CoQ_1 as the electron acceptor to analyze the activity of complex I purified from bovine heart. They proposed an ordered sequential mechanism with CoQ_1 binding as the first step and CoQ_1H_2 releasing as the last step. Hano et al. [39] assumed that the kinetics of complex I obeys an ordered sequential mechanism when they used decylubiquinone (DQ) as the electron acceptor.

Analyzing the same set of experimental results as in this study in the light of a stochastic model based on Gillespie's approach [40] and taking into account the structure (distances) and the midpoint potentials of the reaction centers we showed that the kinetics may not necessarily obey a simple mechanism (ordered or ping-pong) [28]. This is particularly due to the substantial distance (around 90 Å) between the NADH oxidation site and the quinone reduction site and the presence of seven redox reactions in between. It makes the two extreme redox sites (NADH/NAD on the one hand and Q/QH_2 on the other hand) as if they were independent from each other. The stochastic simulations also evidenced a plateau for saturating NADH concentrations (see figures a–j in Fig. S3 to S8). It renders the fit by any equation used in this study slightly inaccurate: at high NADH concentrations the theoretical curves go on increasing weakly, while the experimental rates (as well as the stochastic simulations) are steady and quasi horizontal. We showed that this does not result from a substrate inhibition but simply from the accumulation of electrons in the intermediate redox centers as NADH concentration increases, leading to a sort of electron buffering effect [28].

This can be easily understood in the following way: if the rate of the second half of the mechanism (Q QH_2) is low as compared to the first one (NADH NAD) and to the intermediate redox reactions inside complex I, for instance low Q and high NADH, then the electrons accumulate

Table 3
Competitive/steric and non-competitive inhibition of complex I by quinones. The table lists the results of fitting all the experimental data with an inhibition term in the ER-HMM equation (Eq. (10)) as explained in the text. The fitting method is the same as in Table 2. When there is only one inhibitory constant, it is called K_i and listed in K_{i1} column. The k_b value has been calculated using the Haldane relationship as in Table 2.

Inhibition	RMSD	k_f	k_b	K_{NADH}	K_Q	K_{NAD}	K_{QH_2}	K_{i1}	K_{i2}
	[nmol NADH·min^{-1}·mg^{-1}]			[μM]	[μM]	[μM]	[μM]	[μM]	[μM]
$I_s = 1 + \frac{Q}{K_{i1}} + \frac{QH_2}{K_{i2}}$	151	2185	$7.42 \cdot 10^{-6}$	4.5	14.7	740	46.9	598	25.4
$I_s = 1 + \frac{Q_{tot}}{K_i}$	153	2194	$1.20 \cdot 10^{-6}$	4.5	14.7	743	7.5	576	
$I_{nc} = \frac{1}{1+\frac{Q_{tot}}{K_i}}$	153	2254	$1.21 \cdot 10^{-6}$	4.5	15.1	743	7.6	561	
$I_{nc} = \frac{1}{1+\frac{Q}{K_i}}$	154	2244	$1.07 \cdot 10^{-6}$	4.5	15.0	744	6.7	575	
$I_{nc} = \left(\frac{1}{1+\frac{Q_{tot}}{K_i}}\right)^2$	153	2209	$1.18 \cdot 10^{-6}$	4.5	14.7	740	7.4	1319	
$I_{nc} = \left(\frac{1}{1+\frac{Q}{K_i}}\right)^2$	154	2200	$1.07 \cdot 10^{-6}$	4.5	14.5	741	6.6	1351	
$I_{nc} = \frac{1}{1+\frac{Q}{K_{i1}}+\frac{QH_2}{K_{i2}}}$	152	2236	$1.04 \cdot 10^{-5}$	4.5	15.0	741	65.6	589	29.8
$I_{nc} = \left(\frac{1}{1+\frac{Q}{K_{i1}}+\frac{QH_2}{K_{i2}}}\right)^2$	151	2198	$2.83 \cdot 10^{-5}$	4.5	14.6	737	177	1367	56.8

progressively backwards on the 7–8 FeS centers in between the two half reactions. As soon as one QH_2 molecule is formed, two electrons from some FeS centers are again rapidly available. The limiting step is the release of the previously formed QH_2 molecule and the binding of the new Q molecule which are phenomena much slower than the "flitting" of the electrons between the FeS centers and operating at a constant rate when Q and QH_2 are constants. In other words, when the second half reaction is slower than the first one, there are always two electrons to reduce a Q molecule when present. It is the reason why a plateau is observed in the kinetics particularly at high NADH and low Q.

Another salient feature of our study is that for all the saturable equations (but EMA) the maximal rate constants and the K_M are nearly the same (see Table 2) and well comparable with the data in the literature on beef heart mitochondria complex I. For instance we find a forward maximal rate constant between 1773 and 1910 nmol·NADH·min^{-1}·mg^{-1}. Fato et al. [37] determined on submitochondrial particles for different types of quinone a k_{cat} ranging from 170 to 1560 nmol·NADH·min^{-1}·mg^{-1}. Sherwood and Hirst [41] reported a value of 3100 nmol·NADH·min^{-1}·mg^{-1} and Hano et al. [39] a value of 1860 nmol·NADH·min^{-1}·mg^{-1}. Lower values around 500 nmol·NADH·min^{-1}·mg^{-1} were reported by other authors with different quinone analogs [42].

K_M (NADH) was found in the range of 0.6–2.7 μM on isolated complex I in the presence of different quinone types, among them also decylubiquinone [38,39], always in beef heart mitochondria. For SMP a value of 9.2 μM has been found [37]. Vinogradov [43] reported for K_M (NADH) 7.6 μM and 7.2 μM for coupled and uncoupled SMPs, respectively. Nakashima et al. [38] found a K_M (NADH) around 2 μM depending on Q1 and NAD concentrations. It is well comparable with the values 4.2–6.1 μM we found in our fits.

The values found for K_M (Q) are more variable, due to the different types of quinone that has been used. Fato et al. [37] determined the K_M (Q) for 7 different types of quinones on bovine submitochondrial particles. Their values for decylubiquinone (DQ) were found to be 1.8 and 2.1 μM. A higher value of 24 μM has also been reported in [41]. For complex I isolated from beef heart, values of 4.4–12.9 μM for Q1 and Q2 [38,39,44] have been reported and 51 μM [39] for decylubiquinone. These values are similar to the values between 9.5 and 13.8 found in our fits.

Less data are available with respect to the K_M values of the products and they are more difficult to compare to our values because of their dependence on the rate equation structures. Vinogradov [45] found a K_i value for NAD of 1250 μM on uncoupled SMP, which lies among the K-values we found for the different equations. However, for the reverse reaction under coupled conditions the author reported a K_M of 7.2 μM for NAD. To explain the difference of about three orders of magnitude it was suggested that NAD binds to a different site for the reverse sense. But this large difference may also be due to the equation that has been used for the determination of these values, as we can see on Tables 2 and 3.

With only three independent parameters (instead of five for the other equations, ER-HMM, PPM or OM), the EMA equation is a significantly less precise description of the given data. However, for most data curves EMA is still comparable to the other rate equations, as one can see in Fig. 2 and on Fig. 4 in Supplementary Material. But since the product inhibition by QH_2 and NAD^+ are approximately three orders of magnitude apart, it is obvious that EMA cannot describe accurately the influence of both. Here the fits lead to a good description of the influence of QH_2, but in contrast, in the series where NAD^+ was varied the data description is not satisfactory. For the latter no QH_2 was present which means that the product term in the EMA equation was always 0, with NAD^+ present or not. Hence EMA is not applicable to such an extreme situation

4.3. Inhibition by Q

In our experimental data one can observe an inhibition of complex I at high concentrations of decylubiquinone (Fig. 4). Indeed oxidized quinones have been suspected to exert a negative effect on complex I activity at higher concentrations. Lenaz et al. [46] showed an inhibitory effect by the short chain CoQ analog Q_3 and assumed that there is a need for long chain ubiquinone for a proper functioning of complex I. Other authors reported this inhibition with different types of quinones [37,44]. Grivennikova et al. [18] reported even a very strong inhibition by the short chain ubiquinone. This could suggest the existence of a second inhibitory site for quinone (oxidized) in addition to the substrate site as we already discussed in [28] (see also [41,44,47–50]). Although, there is no evidence of a precise second ubiquinone site, there is the possibility of ubiquinone taking several positions either in the large reaction pocket or on the way leading from the membrane to the reaction site and thus impeding or hindering the access of the ubiquinone substrate by ubiquinol or the release of the ubiquinol product by ubiquinone, well modeled by a steric inhibition either by Q or QH_2. It should be noticed that the inhibitory concentration of Q is rather high (>100 μM) and that 15–20% inhibition is obtained at 350 μM Q. Thus the inhibition term can be presumably neglected in most of the cases.

4.4. Choice of a rate equation

Because all equations but EMA give a similar good fit of our kinetic experiments performed with large variations of the substrates and products, we select the ER-HMM equation to represent complex I activity. It is among the simplest and corresponds to the random bi–bi mechanism. As noted above, the inhibitory term is probably most of the time superfluous. If necessary, it will be added under the form of a noncompetitive inhibition by Q_{tot}. Both types of inhibition (non competitive and steric) give a very comparable inhibitory pattern (Figs. 7 and 8 in Supplementary Material).

$$v = E_t.I_{nc} \cdot \frac{k_f.\frac{NADH}{K_{NADH}}.\frac{Q}{K_Q} - k_b.\frac{NAD}{K_{NAD}}.\frac{QH_2}{K_{QH_2}}}{\left(1+\frac{NADH}{K_{NADH}}+\frac{NAD}{K_{NAD}}\right)\left(1+\frac{Q}{K_Q}+\frac{QH_2}{K_{QH_2}}\right)} \quad (13)$$

with

$$I_{nc} = \left(\frac{1}{1+\frac{[Q_{tot}]}{K_i}}\right) \quad (14)$$

We have shown that this type of equation (ER-HMM) can be used to fit the kinetics of the other complexes of the respiratory chain [51].

In a forthcoming paper we will discuss the introduction of the proton gradient in biothermokinetic rate equations and analyze different approaches with respect to their ability to reproduce OXPHOS data under coupled conditions.

Supplementary data to this article can be found online at http://dx.doi.org/10.1016/j.bbabio.2014.07.013.

Acknowledgements

The authors are indebted to Drs. Joel Lunardi and Gaëlle Hardy for the preparation of mitochondria, to Dr. S. Ransac for fruitful discussions and to Prof. Edda Klipp for her constant support.

References

[1] M. Frenzel, H. Rommelspacher, M.D. Sugawa, N.A. Dencher, Ageing alters the supramolecular architecture of OxPhos complexes in rat brain cortex, Exp. Gerontol. 45 (2010) 563–572.
[2] D.C. Wallace, Mitochondrial DNA mutations in disease and aging, Environ. Mol. Mutagen. 51 (2010) 440–450.
[3] S. DiMauro, E.A. Schon, Mitochondrial disorders in the nervous system, Annu. Rev. Neurosci. 31 (2008) 91–123.
[4] G. Magnus, J. Keizer, Minimal model of b-cell mitochondrial $Ca2^+$ handling, Am. J. Physiol. 273 (1997) C717–C733 (Cell Physiol. 42).
[5] S. Cortassa, M.A. Aon, E. Marban, R.L. Winslow, B. O'Rourke, An integrated model of cardiac mitochondrial energy metabolism and calcium dynamics, Biophys. J. 84 (2003) 2734–2755.
[6] H. Rottenberg, Non-equilibrium thermodynamics of energy conversion in bioenergetics, Biochim. Biophys. Acta 549 (1979) 225–253.
[7] H.V. Westerhoff, K. van Dam, Thermodynamics and Control of Free-energy Transduction, Elsevier, Amsterdam, 1987.
[8] J.W. Stucki, The thermodynamic-buffer enzymes, Eur. J. Biochem. 109 (1980) 257–267.
[9] J.W. Stucki, The optimal efficiency and the economic degrees of coupling of oxidative phosphorylation, Eur. J. Biochem. 109 (1980) 269–283.
[10] B. Korzeniewski, W. Froncisz, Theoretical studies on the control of the oxidative phosphorylation system, Biochim. Biophys. Acta 1102 (1992) 67–75.
[11] B. Korzeniewski, Regulation of ATP supply in mammalian skeletal muscle during resting state → intensive work transition, Biophys. Chem. 83 (2000) 19–34.
[12] B. Korzeniewski, J.-P. Mazat, Theoretical studies on the control of oxidative phosphorylation in muscle mitochondria at different energy demands and oxygen concentrations, Acta Biotheor. 44 (1996) 263–269.
[13] B. Korzeniewski, M. Malgat, T. Letellier, J.-P. Mazat, Effect of binary mitochondria heteroplasmy on respiration and ATP synthesis: implications to mitochondrial diseases, Biochem. J. 357 (2001) 835–842.
[14] R. Bohnensack, Control of energy transformation of mitochondria. Analysis by a quantitative model, Biochim. Biophys. Acta 634 (1981) 203–218.
[15] D.A. Beard, A biophysical model of the mitochondrial respiratory system and oxidative phosphorylation, PLoS Comput. Biol. 1 (2005) 252–264.
[16] S. Helling, M. Hüttemann, R. Ramzan, S.H. Kim, I. Lee, T. Müller, E. Langenfeld, H.E. Meyer, B. Kadenbach, S. Vogt, K. Marcus, Multiple phosphorylations of cytochrome *c* oxidase and their functions, Proteomics 12 (2012) 950–959.
[17] B. Kadenbach, R. Ramzana, L. Wenb, S. Vogt, New extension of the Mitchell Theory for oxidative phosphorylation in mitochondria of living organisms, Biochim. Biophys. Acta 1800 (2010) 205–212.
[18] V.G. Grivennikova, A.N. Kapustin, A.D. Vinogradov, Catalytic activity of NADH ubiquinone oxidoreductase (complex I) in intact mitochondria. Evidence for the slow active/inactive transition, J. Biol. Chem. 276 (2001) 9038–9044.
[19] N. Capitanio, L.L. Palese, G. Capitanio, P.L. Martino, O.M. Richter, B. Ludwig, S. Papa, Allosteric interactions and proton conducting pathways in proton pumping aa3 oxidases: heme a as a key coupling element, Biochim. Biophys. Acta 1817 (2012) 558–566.
[20] K. Yugi, M. Tomita, A general computational model of mitochondrial metabolism in a whole organelle scale, Bioinformatics 20 (2004) 1795–1796.
[21] N. Berndt, S. Bulik, H.-G. Holzhütter, Kinetic modeling of the mitochondrial energy metabolism of neuronal cells: the impact of reduced α-ketoglutarate dehydrogenase activities on ATP production and generation of reactive oxygen species, Int. J. Cell Biol. 2012 (2012), http://dx.doi.org/10.1155/2012/757594 (Article ID 757594, 11 pages).
[22] F. Medja, S. Allouche, P. Frachon, C. Jardel, M. Malgat, B. Mousson de Camaret, A. Slama, J. Lunardi, J.P. Mazat, A. Lombès, Development and implementation of standardized respiratory chain spectrophotometric assays for clinical diagnosis, Mitochondrion 9 (2009) 331–339 (See also http://mitolab.eu/consensus-protocols-for-clinical-diagnosis/) .
[23] A. Cornish-Bowden, J.-H.S. Hofmeyr, Enzyme in context: kinetic characterization of enzymes for systems biology, Biochemist (April 2005) 11–14.
[24] C. Chassagnole, B. Raïs, E. Quentin, D.A. Fell, J.-P. Mazat, An integrated study of threonine pathway enzyme kinetics in *Escherichia coli*, Biochem. J. 356 (2001) 415–423.
[25] J.M. Rohwer, Kinetic modelling of plant metabolic pathways, J. Exp. Bot. 63 (2012) 2275–2292.
[26] I.H. Segel, Rapid equilibrium bireactant systems, in: I.H. Segel (Ed.), Enzyme Kinetics. Behavior and Analysis of Rapid Equilibrium and Steady-state Enzyme Systems, Wiley Classics Library Edition, John Wiley & Sons, New York, ISBN: 978-0-471-30309-1, 1993.
[27] W. Liebermeister, E. Klipp, Bringing metabolic network to life: convenience rate law and thermodynamic constraints, Theor. Biol. Med. Model. 3 (2006) 41.
[28] S. Ransac, M. Heiske, J.-P. Mazat, From in silico to in spectro kinetics of Respiratory Complex I, Biochim. Biophys. Acta 1817 (2012) 1958–1969.
[29] A.L. Smith, Preparation, properties, and conditions for assay of mitochondria: slaughterhouse material, small-scale, Methods Enzymol. 10 (1967) 81–86.
[30] P. Mendes, D. Kell, Non-linear optimization of biochemical pathways: applications to metabolic engineering and parameter estimation, Bioinformatics 14 (1998) 869–883.
[31] V. Henri, Théorie générale de l'action de quelques diastases, CR Acad. Sci. Paris 135 (1902) 916–919.
[32] L. Michaelis, M.L. Menten, Die Kinetic der Invertinwirkung, Biochem. Z. 49 (1913) 333–369.
[33] G.E. Briggs, J.B.S. Haldane, A note on the kinetics of enzyme action, Biochem. J. 19 (1925) 338–339.
[34] U. Deichmann, S. Schuster, J.-P. Mazat, A. Cornish-Bowden, Commemorating the 1913 Michaelis–Menten paper Die Kinetik der Invertinwirkung: three perspectives, FEBS J. 281 (2014) 435–463.
[35] W. Liebermeister, J. Uhlendorf, E. Klipp, Modular rate laws for enzymatic reactions: thermodynamics, elasticities and implementation, Bioinformatics 26 (2010) 1528–1534.
[36] C.S. Pillay, J.-H.S. Hofmeyr, B.G. Olivier, J.L. Snoep, J.M. Rohwer, Enzymes or redox couples? The kinetics of thioredoxin and glutaredoxin reactions in a systems biology context, Biochem. J. 417 (2009) 269–275.
[37] R. Fato, E. Estornell, S. Di Bernardo, F. Pallotti, G. Parenti Castelli, G. Lenaz, Steady-state kinetics of the reduction of coenzyme Q analogs by complex I (NADH:ubiquinone oxidoreductase) in bovine heart mitochondria and submitochondrial particles, Biochemistry 35 (1996) 2705–2716.
[38] Y. Nakashima, K. Shinzawa-Itoh, K. Watanabe, K. Naoki, N. Hano, S. Yoshikawa, Steady-state kinetics of NADH:coenzyme Q oxidoreductase isolated from bovine heart mitochondria, J. Bioenerg. Biomembr. 34 (2002) 11–19.
[39] N. Hano, Y. Nakashima, K. Shinzawa-Itoh, S. Yoshikawa, Effect of the side chain structure of coenzyme Q on the steady state kinetics of bovine heart NADH: coenzyme Q oxidoreductase, J. Bioenerg. Biomembr. 35 (2003) 257–265.
[40] D.T. Gillespie, Exact stochastic simulation of coupled chemical reactions, J. Phys. Chem. 81 (1977) 2340–2361.
[41] S. Sherwood, J. Hirst, Investigation of the mechanism of proton translocation by NADH:ubiquinone oxidoreductase (complex I) from bovine heart mitochondria: does the enzyme operate by a Q-cycle mechanism? Biochem. J. 400 (2006) 541–550.
[42] M. Ohshima, H. Miyoshi, K. Sakamoto, K. Takegami, J. Iwata, K. Kuwabara, H. Iwamura, T. Yagi, Characterisation of the ubiquinone reduction site of mitochondrial complex I using bulky synthetic ubiquinones, Biochemistry 37 (1998) 6436–6644.
[43] A.D. Vinogradov, Kinetics, control, and mechanism of ubiquinone reduction by the mammalian respiratory chain-linked NADH-ubiquinone reductase, J. Bioenerg. Biomembr. 25 (1993) 367–375.
[44] Y. Nakashima, K. Shinzawa-Itoh, K. Watanabe, K. Naoki, N. Hano, S. Yoshikawa, The second coenzyme Q1 binding site of bovine heart NADH: coenzyme Q oxidoreductase, J. Bioenerg. Biomembr. 34 (2002) 89–94.
[45] A.D. Vinogradov, Catalytic properties of the mitochondrial NADH–ubiquinone oxidoreductase (complex I) and the pseudo-reversible active/inactive enzyme transition, Biochim. Biophys. Acta 1364 (1998) 169–185.
[46] G. Lenaz, P. Pasquali, E. Bertoli, G. Parenti-Castelli, The inhibition of NADH oxidase by the lower homologs of coenzyme Q, Arch. Biochem. Biophys. 169 (1975) 217–226.

[47] T. Ohnishi, J.E. Johnson Jr., T. Yano, R. Lobrutto, W.R. Widger, Thermodynamic and EPR studies of slowly relaxing ubisemiquinone species in the isolated bovine heart complex I, FEBS Lett. 579 (2005) 500–506.
[48] S. Magnitsky, L. Toulokhonova, T. Yano, V.D. Sled, C. Hägerhäll, V.G. Grivennikova, D. S. Burbaev, A.D. Vinogradov, T. Ohnishi, EPR characterization of ubisemiquinones and iron–sulfur cluster N2, central components of the energy coupling in the NADH–ubiquinone oxidoreductase (complex I) in situ, J. Bioenerg. Biomembr. 34 (2002) 193–208.
[49] R. Baradaran, J.M. Berrisford, G.S. Minhas, L.A. Sazanov, Crystal structure of the entire respiratory complex I, Nature 494 (2013) 443–448.
[50] C. Hunte, V. Zickermann, U. Brandt, Functional modules and structural basis of conformational coupling in mitochondrial complex I, Science 329 (2010) 448–451.
[51] M. Heiske, (PhD thesis) http://www.bu.u-bordeaux2.fr/babordplus.php?special=these.